Gas-Phase Electronic Spectrum of the Tropyl C_7H_7 Radical†

T. Pino, F. Güthe, H. Ding, and J. P. Maier*

Department of Chemistry, University of Basel, Klingelbergstrasse 80, CH-4056, Basel, Switzerland

Received: April 5, 2002; In Final Form: July 5, 2002

One color resonance enhanced two photon ionization spectra of the tropyl C_7H_7 and C_7D_7 radicals were recorded in a molecular beam. Tropyl was produced in a supersonic plasma source using different precursors to identify its vibronic bands. The vibronic system is assigned to the $^2E_3'' \leftarrow X^2E_2''$ electronic transition with origin near 25 719 cm^{-1}. It covers 6 000 cm^{-1} revealing a large change of geometry due to a Jahn−Teller distortion in both the ground and the excited states. Ab initio calculations were carried out on the Jahn−Teller configurations to guide the assignment.

I. Introduction

The tropylium (cycloheptatrienyl) cation $C_7H_7^+$ is a prototype aromatic cation because of the stabilization due to the filled π -electron sextet according to the $(4n + 2)$ Hückel rule. As a result the ionization potential is only 6.23 eV for the neutral tropyl radical C_7H_7.[1] Tropylium is an important fragmentation channel product in competition with the benzyl cation in mass spectrometric studies of aromatic derivatives.[2−5] This is one of the most studied reactions in the field of gas-phase ion chemistry and tropylium is considered as the most stable isomer. The tropyl radical has been poorly investigated compared to neutral benzyl.[6] Though the latter is more stable by only 40 kJ/mol,[7] tropyl is believed to convert rapidly to benzyl. Further data on tropyl may aid the investigation of such reactions by laser-based diagnosis. Photolytic[8] and pyrolytic[1] methods have been used to produce tropyl from bitropyl and photolysis of cycloheptatriene was found to produce the benzyl radical.[9] A chemical method via the reaction of cycloheptatriene with atomic fluorine or chlorine in a flow reactor have been used.[10] In the present study the source is a supersonic expansion coupled to an electric discharge. With this technique the chemical products in the plasma were found to be sampled at an early stage allowing the detection of a number of unusual intermediates.[11]

Tropyl has a X^2E_2'' ground state in the D_{7h} symmetry group with $...(a_2'')^2(e_1'')^4(e_2'')^1(e_3'')^0$ electronic configuration.[12] It is the only molecule known to belong to this group of symmetry. Because of the singly occupied e_2'' orbital, this radical is subject to a Jahn−Teller (JT) distortion. The ground state has been investigated by ESR spectroscopy,[13] photoelectron spectroscopy,[14] and ab initio calculations.[15] The photoelectron spectrum suggests a highly fluxional ground state which is consistent with the ESR results showing seven equivalent protons and a uniform spin distribution. These observations support JT instability for the X^2E_2'' ground state. Electron excitations lead to a number of states with $...(e_3'')^1$ and $...(e_1'')^3(e_2'')^2$ configurations. A Hückel molecular orbital calculation yielded excitation energies of 27 000 cm^{-1} to the $^2E_3''$ and 34 000 cm^{-1} to the $^2E_1''$ state.[12] An early semiempirical calculation (in D_{7h}) predicted values of 32 880 ($^2E_2''$), 34 400 ($^2E_3''$), 40 800 ($^2E_1''$) and 51 300 cm^{-1} ($^2E_2''$) for the electronic excited states.[16] Except for $^2E_2'' \leftarrow X^2E_2''$, all these electronic transitions are dipole-allowed. Previous work on the electronic spectroscopy of tropyl focused on the region above 35 000 cm^{-1}, and only Rydberg states have been found by direct absorption[8] and [2+1]-resonance enhanced multiphoton (REMPI) spectroscopy in the visible.[10]

In this article, a resonant one color two photon ionization technique was applied in the near-UV range covering the expected positions of the first electronic transitions of tropyl. Ab initio calculations are carried out to guide the interpretation of the spectrum.

II. Experimental Section

The setup of the REMPI apparatus has been described in a previous paper.[11] It consists of a time-of-flight mass spectrometer (TOF) coupled to a molecular beam extracted from a supersonic plasma source. The tropyl radical is formed in a gas pulse of an hydrocarbon precursor seeded in Ar coupled to a pulsed electrical discharge (∼100 μs; 500−1000 V). This source has been shown to produce a large number of cold hydrocarbon molecules.[11] The molecular beam is then intersected by the laser in the extraction zone of the TOF.

Resonance-enhanced one-color two-photon ionization (R2PI) spectra were recorded in the 400−277 nm range with the frequency doubled output of an YAG pumped dye laser (bandwidth ≃ 0.15 cm^{-1}) and the output of a dye laser (bandwidth ≃0.1 cm^{-1}) pumped by an excimer laser for the longer wavelengths. Typical laser pulse energies are 1−2 mJ. The output of a F_2 excimer laser running at 157 nm (7.9 eV) is used to probe the neutral distribution by a multiphoton ionization technique and the resulting mass spectrum is largely dominated by the direct ionization process.

III. Results and Structural Assignment

A. Identification of the Carrier. The R2PI spectra recorded at mass 91 using benzene and mass 98 with d_6-benzene as precursor gases (∼0.5% in Ar) are shown in Figure 1. The plasma source was operated under conditions to produce a rich mass spectrum, signature of extensive chemistry.[11] The observed vibronic system is rather complex and covers a wide wavelength range. Identification of the molecule(s) giving rise to the observed spectrum in the benzene discharge is not straightforward because many different isomers of C_7H_7 exist.[14] The

† Part of the special issue "Jack Beauchamp Festschrift".

* Corresponding author. E-mail: J.P. Maier@unibas.ch

10.1021/jp020910y CCC: $22.00
Published on Web 08/13/2002

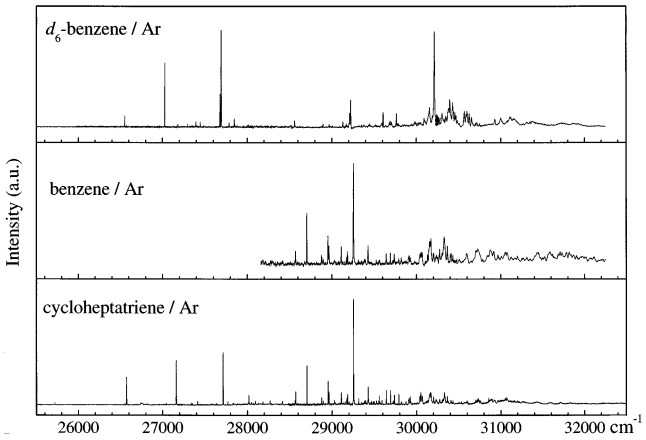

Figure 1. Resonant two photon one color ionization spectra of the C_7H_7 and C_7D_7 species in the gas phase. The gas mixture employed in the discharge is indicated.

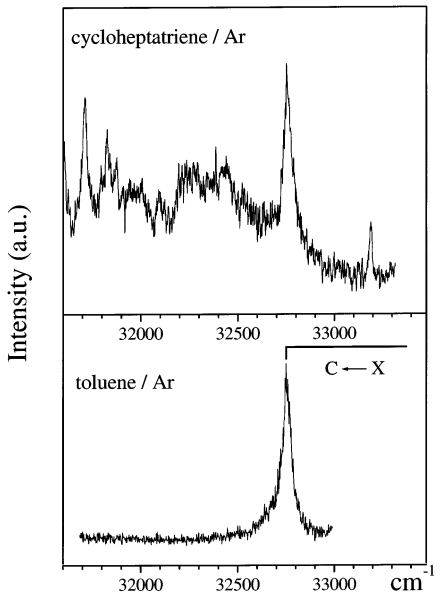

Figure 2. Close-up of the energy region of the $C^2A_2 \leftarrow X^2B_2$ electronic transition in benzyl. The spectra were recorded in toluene-containing and cycloheptatriene-containing discharges. The additional vibronic system is clearly absent in the former.

known benzyl radical electronic spectrum[6] does not correspond to the observed bands. Spectra were measured using different precursors in order to identify the band of the tropyl radical.

A mixture of cycloheptatriene seeded in Ar was used with a low concentration (0.02%) to avoid rich chemistry. The plasma source was operated in a way such that only one mass peak corresponding to C_7H_7 is produced (the first unimolecular reaction channel). The voltage (500 V; 80 μs) was set to the lowest value necessary to trigger the discharge. The resulting spectrum is shown in Figure 1. The known electronic $C^2A_2 \leftarrow X^2B_2$ transition of benzyl has its origin band at 32 760 cm^{-1}.[6,17] It is detected at the blue end (Figure 2). The other vibronic systems are observed using benzene as the precursor (Figure 1). The signal-to-noise ratio is much better using cycloheptatriene than benzene as the hydrocarbon precursor but a one to one correspondence is found between the two spectra. These results lead to the assignment of the band system to one isomer, apart from the bands belonging to benzyl. Because tropyl has an ionization potential (IP) equal to 6.23 eV,[1] below the upper limit of 6.38 eV accessible to the present R2PI experiment, and as it is the most probable product formed in this discharge prior to a fast isomerization to benzyl, this isomer is identified as the carrier of the measured electronic transition.

TABLE 1: The Main Vibronic Bands (±3 cm^{-1}) Observed in the $A^2E_3'' \leftarrow X^2E_2''$ Gas-Phase Electronic Spectrum of C_7H_7 and C_7D_7 Measured by Resonant Two-Photon Ionization Technique

C_7H_7		C_7D_7		
ν (cm^{-1})	$\Delta\nu$ (cm^{-1})	ν (cm^{-1})	$\Delta\nu$ (cm^{-1})	assignment
25 719	0		0	0_0^0
26 573	854	26 553	866	2_0^1
27 159	1 440	27 027	1 340	$\vert^1/2,n_1\rangle$
		27 679	1 992	
27 711	1 991	27 693	2 006	$\vert^1/_2,n_2\rangle$
28 018	2 299			$2_0^1\vert^1/_2,n_1\rangle$
28 269	2 550			6_0^2
28 571	2 852	28 559	2 872	$2_0^1\vert^1/_2,n_2\rangle$
28 704	2 985			$\vert^1/_2,n_3\rangle$
28 877	3 158			$2_0^2\vert^1/_2,n_1\rangle$
28 954	3 235			$13_0^1 + 8_0^2$
28 965	3 246	28 897	3 210	$13_0^1 + 8_0^2$
29 110	3 391			
29 184	3 465	29 129	3 442	
29 254	3 535	29 222	3 535	$\vert^1/_2,n_4\rangle$
29 427	3 708			$2_0^2\vert^1/_2,n_2\rangle$
29 558	3 839			$2_0^1\vert^1/_2,n_3\rangle$
29 641	3 922	29 607	3 920	
29 691	3 972			
29 737	4 018	29 689	4 002	$2_0^3\vert^1/_2,n_1\rangle$
29 791	4 072			
29 821	4 102	29 763	4 076	$8_0^2 2_0^1$
29 912	4 193	29 988	4 301	
30 055	4 336	30 091	4 404	
30 170	4 451	30 213	4 526	
30 328	4 609	30 305	4 618	
		30 393	4 706	
30 507	4 788	30 430	4 743	
30 593	4 874	30 568	4 881	
30 726	5 007	30 719	5 032	
30 877	5 158	30 931	5 244	
31 050	5 331	31 002	4 449	
31 195	5 476	31 160	5 315	
31 312	5 593	31 309	5 622	

A mixture of toluene (0.03%) seeded in Ar was also used with the source conditions as in the experiment with cycloheptatriene. The IP of the benzyl radical (the first unimolecular reaction channel) is 7.25 eV and therefore can be observed in the mass spectrometric studies with the F_2 laser. However, the complex vibronic system recorded using benzene as the precursor is not observed and only the $C^2A_2 \leftarrow X^2B_2$ electronic transition of benzyl is detected. A close-up of the spectra in the region of this transition is shown in Figure 2. Tropyl is not formed in this discharge implying that tropyl isomerizes to benzyl and the reverse process does not occur. It appears that the source used in our experiment quenches this isomerization with the aid of the supersonic expansion which cools the products.

B. Spectroscopic Results. The frequencies of the main vibronic bands are given in Table 1. The center of the bands were determined visually and no obvious positions of the maxima in the high energy region can be determined because of the multiline structures. The origin band of the C_7H_7 electronic spectrum is at 25 719 ± 3 cm^{-1}.

The vibronic system is extensive indicating a large geometry change between the two involved electronic states. Also deuteration strongly affects the high energy region of the spectra. The relative intensities shown in Figure 1 should be considered qualitatively because many dyes were used to cover the whole range. In the spectra no vibrational progression can be identified,

TABLE 2: Optimized Geometries (in Ångstroms) of the Tropyl Radical, Neutral, and Cation, at the CASSCF(7,7)/6-31G* Level[a]

		cation	neutral			
		X^1A_1'	$^2B_1(X^2E_2'')$	$^2A_2(X^2E_2'')$	$^2B_1(A^2E_3'')$	$^2A_2(A^2E_3'')$
energy (H)		−268.98206	−269.16732	−269.16732	−269.02518	−269.02518
ϵ_{JT} (eV)		0.0	0.213	0.213	0.365	0.365
C−C bond	1−2	1.396	1.421	1.3954	1.4649	1.4022
	2−3	1.396	1.3736	1.4444	1.448	1.429
	3−4	1.396	1.4598	1.3598	1.4103	1.459
	4−5	1.396	1.3554	1.4654	1.4	1.468
C−H bond	1−8	1.0747	1.0749	1.0774	1.0733	1.0766
	2−9	1.0747	1.0774	1.075	1.0736	1.0757
	3−10	1.0747	1.0755	1.077	1.0751	1.0743
	4−11	1.0747	1.0767	1.076	1.0764	1.0732

[a] Only the bond lengths are given. Carbon 1 is located on the C_2 axis in the C_{2v} group and the others (2−7) are numbered clockwise; the hydrogen 8 is bound to the carbon 1 and the others (9−14) are numbered clockwise.

though one mode with a frequency of 859 (866) cm^{-1} for $C_7H(D)_7$ appears in combination with others.

The band profiles vary but follow a general trend consisting of an increasing broadness with excess of vibrational energy above the electronic origin (fwhm up to several cm^{-1}). These line shapes are not dependent on experimental conditions and the broadening in the high energy region is intrinsic. This is attributed to intramolecular vibrational redistribution (IVR) reinforced by the JT coupling. This trend is even more pronounced in the case of C_7D_7 and is understood as due to the increase in the density of states available for the IVR process.

IV. Calculations of the Jahn−Teller Configurations

A. General Features. Theoretical calculations have been carried out on the tropyl radical. All ab initio calculations were undertaken using the MOLPRO package[18] and GAUSSIAN 98 suite of programs[19] for CASSCF and B3LYP calculations respectively, with the Pople type basis sets.[20] At the CASSCF level of theory, these include seven electrons in the seven π orbitals, abbreviated CAS(7,7). A comparable level has been used recently to study the cyclopentadienyl molecule.[21]

Unlike the cationic ground state X^1A_1', the neutral one X^2E_2'' is subject to a Jahn−Teller (JT) distortion. The linear E⊗e JT effect is considered for tropyl, as has been used previously for the benzene cation and the cyclopentadienyl radical.[22] The adiabatic potential energy surface (APES) of the two states becomes a surface of revolution (the "Mexican hat") when plotted versus the two coordinates that lift the degeneracy present at the D_{7h} geometry.[22] The degeneracy point becomes a conical intersection. The D_{7h} group possesses several subgroups and tropyl ground and first excited states are found to split into two planar components (the JT configurations) $^2B_1$ and $^2A_2$ in the C_{2v} group. Therefore the calculations were carried out in the C_{2v} symmetry group although tropyl belongs to D_{7h}.

B. Ground State. The ground-state structure of the tropylium cation was calculated at the CAS(7,7)/6-31G* level. The bond lengths are reported in Table 2. The predicted structure is in good agreement with the experimental one ($R_{C-C} = 1.40 \pm 0.02$ Å[23]). This D_{7h} geometry is used to approximate the degeneracy point of the neutral electronic states. There was no attempt to obtain the geometry at the conical intersections in the neutral. This approximation allows an estimation of the JT stabilization energy (ϵ_{JT}) which is the difference between the lowest JT configuration(s) and the degeneracy point.

JT configurations of the neutral tropyl in its ground state were first obtained at the CAS(7,7)/6-31G* level. The geometries are reported in Table 2. Two minima of $^2B_1$ and $^2A_2$ symmetries are found. These are calculated to be isoenergetic as was found in a previous study.[14] Further calculations show that the molecule remains planar and distortions down to C_s symmetry do not occur. Geometry optimization and frequency calculations at the B3LYP/6-31G** level starting at the CAS(7,7) $^2B_1$ geometry predict a stationary point with the same symmetry while a saddle point possessing $^2A_2$ symmetry is found starting with the CAS(7,7) $^2A_2$ geometry (Table 3). However, these two are almost isoenergetic (Table 3). At the CAS(7,7)/6-311+G* level a difference of 20 meV is found between the two components and MP2/6-31G** calculations predict 65 meV.[15] This discrepancy points out the difficulty in extracting JT parameters from ab initio calculations and no definitive conclusion on the existence of a barrier to the pseudorotation can be given. Nevertheless a small difference between the two JT configurations is consistent with the photoelectron spectrum[14] and the ESR results.[13] The JT distortion results in a C−C bond alternation (ΔR_{C-C} up to 0.07 Å) while it only slightly affects the C−H bond length. ϵ_{JT} is estimated to be 213 and 149 meV within the CASSCF and B3LYP calculations.

In the work of Lee and Wright[15] it is shown that the vibration ω_{32} (ω_{33} in their notation) of b_2 symmetry, in the X^2B_1 state, is strongly dependent on the level of theory employed and is predicted to have a very low value. B3LYP/6-31G** geometry optimization in the C_s group starting from the $^2A_2$ geometry leads to a stationary point with $\omega_{32} = 98$ cm^{-1}, and the predicted structure is indistinguishable from the C_{2v} one. In fact mode ω_{32} correlates to a vibration of e_3' symmetry in D_{7h} and removes the degeneracy of the ground X^2E_2'' state in the frame of the linear E⊗e JT problem. It appears to correspond to the pseudorotation coordinate[22,24] and ω_8, which is degenerate with ω_{32} at the D_{7h} geometry (Table 3), to the radial motion. These results are similar to ab initio calculations performed on the benzene cation[25,26] and c-$C_5H_5^{+}$ [27] and point out that mostly this e_3' mode is JT active. This vibration has different contributions from the carbon skeleton (C−C stretch) and the C−H wagging motion between the different charge states, the former being much more important for the neutral as reflected by the large reduced mass (9 amu). The other three modes of e_3' symmetry in D_{7h} group are dominated by a C−H motion in the neutral as well as in the cation ground state.

C. Excited States. At first excited states calculations were performed at the CAS(7,7)/6-31G* level using the D_{7h} structure of the cation. The first two excited states in the C_{2v} group are dominated by the $...(e_3'')^1$ and $...(e_1'')^3(e_2'')^2$ electronic configurations in D_{7h}, respectively. This is in agreement with the Hückel molecular orbital (HMO) results and the symmetries of the excited states follow this work.[12] These calculations indicate that the C−C bond length of these excited states at the

TABLE 3: Optimized Geometries (in Å) of the Tropyl Radical, Neutral, and Cationic, at the B3LYP/6-31G Level[a]**

	cation	neutral	
	X^1A_1'	$^2B_1(X^2E_2'')$	$^2A_2(X^2E_2'')$
energy (H)	−270.67857	−270.899018	−270.899011
C1−C2 bond	1.3985	1.4159	1.3950
C2−C3 bond	1.3985	1.3770	1.4352
C3−C4 bond	1.3985	1.4495	1.3647
C4−C5 bond	1.3985	1.3600	1.4545
$\omega_1(a_1)$	439 (e_2')	419	446
ω_2	880 (a_1')	850	850
ω_3	898 (e_3')	914	914
ω_4	1 015 (e_1')	969	965
ω_5	1 251 (e_2')	1250	1193
ω_6	1 313 (e_3')	1291	1290
ω_7	1 519 (e_1')	1486	1483
ω_8	1 569 (e_3')	1614	1634
ω_9	1 637 (e_2')	1666	1552
ω_{10}	3 187 (e_3')	3144	3144
ω_{11}	3 197 (e_2')	3168	3150
ω_{12}	3 205 (e_1')	3186	3183
ω_{13}	3 210 (a_1')	3195	3195
$\omega_{14}(a_2)$	225 (e_3'')	290	160
ω_{15}	564 (e_3'')	567	566
ω_{16}	891 (e_1'')	768	757
ω_{17}	1 061 (e_2'')	994	844
ω_{18}	1 079 (e_2'')	1009	994
$\omega_{19}(b_1)$	225 (e_3'')	161	290
ω_{20}	564 (e_3'')	517	516
ω_{21}	664 (a_2'')	656	656
ω_{22}	891 (e_1'')	758	770
ω_{23}	1 061 (e_2'')	845	985
ω_{24}	1 079 (e_2'')	985	1009
$\omega_{25}(b_2)$	439 (e_2')	446	420
ω_{26}	898 (e_3')	905	906
ω_{27}	1 015 (e_1')	973	978
ω_{28}	1 255 (e_2')	1193	1250
ω_{29}	1 313 (e_3')	1309	1309
ω_{30}	1 441 (a_2')	1420	1419
ω_{31}	1 519 (e_1')	1490	1494
ω_{32}	1 569 (e_3')	40	−48
ω_{33}	1 637 (e_2')	1561	1653
ω_{34}	3 187 (e_3')	3144	3145
ω_{35}	3 196 (e_2')	3151	3168
ω_{36}	3 205 (e_1')	3184	3186

[a] Only the C−C bond lengths are given. The symmetry of the vibrational modes is given in the C_{2v} group together with the corresponding one in D_{7h} in parentheses used by Lee et al.[15] (The harmonic frequencies are unscaled.)

degeneracy point is not that different from the cationic one because the two C_{2v} components possess the same energy. An increase of the active space reveals differences pointing out that CAS(7,7) calculations have to be considered as preliminary investigations. A higher level is necessary to obtain quantitatively reliable values.

Geometries of the two components arising from the first electronic excited state, A^2E_3'' in the D_{7h} group, were optimized at the CAS(7,7)/6-31G* level. This state splits into a $^2B_1$ and a $^2A_2$ component which are found to be isoenergetic. Further calculations show that the molecule remains planar and distortions down to C_s symmetry do not occur. ϵ_{JT} is estimated to be 365 meV, larger than that in the ground state. Unlike the ground state these two JT configurations do not show C−C bond alternation. The results are reported in Table 2. In this case the e_1' modes remove the degeneracy of the E_3'' excited state in the linear E⊗e JT effect.

All the calculated geometries were used for single point calculations of the vertical excitation energies at the CAS(7,7)/6-311+G* level. ϵ_{JT} are comparable to the results obtained with the smaller basis set used for the geometry optimization and indeed the vertical excitation energies are found to be similar. The lowest calculated adiabatic excitation energy (3.85 eV) is 0.66 eV higher than the observed electronic transition (3.19 eV), but the HMO result is rather close (3.35 eV) to the observed spectrum. Because the molecule possesses isoenergetic JT configurations in the C_{2v} group, the assignment of the observed electronic transition, $A^2E_3'' \leftarrow X^2E_2''$, is given in D_{7h} symmetry. The next allowed electronic transition is predicted ∼1 eV higher than the first one and does not lie in the covered range.

V. Vibronic Analysis

Tentative assignment of the bands in the $A^2E_3'' \leftarrow X^2E_2''$ electronic spectrum of C_7H_7 is based on the ab initio harmonic frequencies of the ground state. These are reported in Table 1. Both states involved in the transition are JT distorted but the theoretical calculations show that apart from the JT active coordinates the other frequencies remain comparable in different components. The notation uses the numbering of the frequencies reported in Table 3 for the non-JT active coordinates in the excited state. Only the a_1 symmetric modes in the C_{2v} group are considered. The electronic origin of C_7H_7 is tentatively assigned to the weak band at 25 719 ± 3 cm^{-1}. It confers the most sensible assignment of the whole spectrum. The corresponding origin band in the C_7D_7 spectrum is not observed because of poorer signal-to-noise ratio achieved in the experiment, and perhaps a weaker Franck−Condon factor.

At first the totally symmetric mode ν_2, ring-breathing motion, is identified with a frequency of 854 ± 5 cm^{-1}. This mode is observed in combination with the other active modes. As its frequency in the spectrum of C_7D_7 is 866 cm^{-1}, the origin band is expected at 25 687 ± 10 cm^{-1}. This vibration was also observed in electronic transitions to Rydberg states and in the ground state of the cation, with frequencies at 862 ± 6 cm^{-1} [10] and 868 cm^{-1}, respectively.

Because the modes of e_3' symmetry are JT active in the ground state their excitation in double quanta are expected. According to the ab initio calculations ν_8 is the most JT active mode in the ground state. Two close-lying bands observed with a rather strong intensity are assigned to the transitions involving ν_8, leading to a frequency of 1 620 ± 10 cm^{-1} in the excited state. Another band involving mode ν_6 is also assigned and its inferred frequency is 1 275 ± 10 cm^{-1}.

The large change of geometry implied by the extended vibronic system, the lack of obvious vibrational progressions and the difference upon deuteration are considered clear signatures of the JT distortion. This is consistent with the ab initio calculations revealing that completely different deformations are involved in the ground and excited states. In addition pseudo-JT effect might play a role in the vibronic coupling in tropyl due to the proximity of the excited states. The theoretical calculations provide some clues for further interpretation. In the cationic ground state ν_8 has the largest reduced mass (7.46 uma) for modes of e_3' symmetry and it is predicted to be the dominant JT active mode. In the A^2E_3'' state the calculated JT configurations reveal also a distortion of the carbon skeleton. Modes ν_4 and ν_7 are degenerate with ν_{27} and ν_{31} in the D_{7h} group, respectively, and are JT active in this state. They possess rather small reduced mass (2.3 and 1.54 uma, respectively) but still the largest in this symmetry. The main contribution to the JT stabilization should be due to the coupling through mode ν_4 but, unlike in the ground state, a second mode (ν_7) is clearly involved. Thus the analysis cannot be restricted to one mode

analysis and a fit of the JT parameters (frequencies and coupling constants) was not attempted owing to the small numbers of identified lines to provide reliable values. The level notation in Table 1 is $|j,n_i\rangle$[28] for the bands attributed to transition to eigenstates resulting from the JT distortion. The selection rule is $\Delta j = 0$ and because the bands originate from the vibrationless level of the ground state (no hot bands could be identified) only levels with $j = {}^1/_2$ are observed. Therefore the levels are simply labeled with $|{}^1/_2,n_i\rangle$ where i just numbers the strongest bands. In the high energy region the spectral congestion and line-broadening preclude assignments.

VI. Conclusions

The lowest allowed electronic transition of the tropyl radical has been observed in the gas phase. As found for the benzene cation family,[22] ionic coronene,[29] cyclopentadienyl C_5H_5,[21,30] and others,[22,28] the linear E⊗e JT effect is responsible for a distortion of the carbon skeleton away from the highest symmetry D_{7h} for the tropyl radical. The calculated JT configurations reveal different types of distortion in the ground and excited states. A fit of the spectra has not been attempted and the interpretation is not complete. Additional experiments such as laser induced fluorescence may provide fruitful data as well as ab initio calculations of spectroscopically observable parameters, as has been the case for the cyclopentadienyl radical.[21]

The tropyl radical has been observed in a supersonic plasma source operated under different conditions. In the benzene containing discharge several reaction steps for its production are necessary and conditions were chosen favoring rich plasma chemistry. As a result no benzyl is detected. In the cycloheptatriene discharge both isomers are detected but from toluene only benzyl. This suggests that the reaction route involving cations dominate the plasma chemistry. Tropylium cation is the most stable isomer and is preferentially produced. Neutral C_7H_7 is produced by its neutralization. The cooling provided by the supersonic expansion is quenching the reaction before isomerization pointing out the capability of this source to produce transient species and that neutralization is related to the cooling.

Acknowledgment. This work was supported by the Swiss National Science Foundation (Project 20-63459.00).

References and Notes

(1) Koeni, T.; Chang, J. *J. Am. Chem. Soc.* **1978**, *100*, 2240.

(2) Traeger, J. C.; McLoughlin, R. G. *Int. J. Mass Spectrom. Ion Phys.* **1978**, *27*, 319.

(3) Schwell, M.; Dulieu, F.; Gee, C.; Jochims, H. W.; Chotin, J. L.; Baumgärtel, H.; Leach, S. *Chem. Phys.* **2000**, *260*, 261 and references therein.

(4) Moon, J. H.; Choe, J. C.; Kim, M. S. *J. Phys. Chem. A* **2000**, *104*, 458.

(5) Smith, B. J.; Hall, N. E. *Chem. Phys. Lett.* **1997**, *279*, 165.

(6) Yao, J.; Bernstein, E. *J. Chem. Phys.* **1997**, *107*, 3352 and references therein.

(7) Lias, S. G.; Bartmess, J. E.; Holmes, J. L.; Levin, R. D.; Liebman, J. F. *J. Chem. Phys. Ref. Data* **1988**, *17*, Suppl. 1.

(8) Thrush, B. A.; Zwolenik, J. J. *Faraday Discuss. Chem. Soc.* **1963**, *35*, 196.

(9) Thrush, B. A.; Zwolenik, J. J. *Bull. Soc. Chim. Belg.* **1962**, *71*, 642.

(10) Johnson, R. D. *J. Chem. Phys.* **1991**, *95*, 7108.

(11) Güthe, F.; Ding, H.; Pino, T.; Maier, J. P. *Chem. Phys.* **2001**, *269*, 347.

(12) Cotton, F. A. *Chemical Applications of Group Theory*; Wiley-Interscience: New York: 1990.

(13) Silverstone, H. J.; Wood, D. E.; McConnell, H. M. *J. Chem. Phys.* **1964**, *41*, 2311 and references therein.

(14) Gunion, R. F.; Karney, W.; Wenthold, P. G.; Borden, W. T.; Lineberger, W. C. *J. Am. Chem. Soc.* **1996**, *118*, 5074.

(15) Lee, E. P. F.; Wright, T. G. *J. Phys. Chem. A* **1998**, *102*, 4007.

(16) Longuet-Higgins, H. C.; McEvens, K. L. *J. Chem. Phys.* **1957**, *26*, 719.

(17) Eiden, G.; Weisshaar, J. C. *J. Chem. Phys.* **1996**, *104*, 8896.

(18) MOLPRO is a package of ab initio programs written by H.-J. Werner and P. J. Knowles, with contributions from others: see www.tc.bham.ac.uk/molpro.

(19) Frisch, M. J.; Trucks, G. W.; Schlegel, H. B.; Scuseria, G. E.; Robb, M. A.; Cheeseman, J. R.; Zakrzewski, V. G.; Montgomery, J. A., Jr.; Stratmann, R. E.; Burant, J. C.; Dapprich, S.; Millam, J. M.; Daniels, A. D.; Kudin, K. N.; Strain, M. C.; Farkas, O.; Tomasi, J.; Barone, V.; Cossi, M.; Cammi, R.; Mennucci, B.; Pomelli, C.; Adamo, C.; Clifford, S.; Ochterski, J.; Petersson, G. A.; Ayala, P. Y.; Cui, Q.; Morokuma, K.; Malick, D. K.; Rabuck, A. D.; Raghavachari, K.; Foresman, J. B.; Cioslowski, J.; Ortiz, J. V.; Stefanov, B. B.; Liu, G.; Liashenko, A.; Piskorz, P.; Komaromi, I.; Gomperts, R.; Martin, R. L.; Fox, D. J.; Keith, T.; Al-Laham, M. A.; Peng, C. Y.; Nanayakkara, A.; Gonzalez, C.; Challacombe, M.; Gill, P. M. W.; Johnson, B. G.; Chen, W.; Wong, M. W.; Andres, J. L.; Head-Gordon, M.; Replogle, E. S.; Pople, J. A. *Gaussian 98*; Gaussian, Inc.: Pittsburgh, PA, 1998.

(20) Ditchfield, R.; Hehre, W. J.; Pople, J. A. *J. Chem. Phys.* **1971**, *54*, 724.

(21) Applegate, B. E.; Miller, T. A.; Barckholtz, T. A. *J. Chem. Phys.* **2001**, *114*, 4855.

(22) Bersuker, I. B. *Chem. Rev.* **2001**, *101*, 1067 and references therein.

(23) Clark, G. R.; Palenik, G. J. *J. Organomet. Chem.* **1973**, *50*, 185.

(24) Herzberg, G. *Molecular Spectra and Molecular Structure*; Van Nostrand: Princeton, 1966; Vol. III.

(25) Linde, R.; Müller-Dethlefs, K.; Wedum, E.; Haber, K.; Grant, E. R. *Science* **1996**, *271*, 1698.

(26) Müller-Dethlefs, K.; Peel, J. B. *J. Chem. Phys.* **1999**, *111*, 10550.

(27) Lee, E. P. F.; Wright, T. G. *Phys. Chem. Chem. Phys.* **1999**, *1*, 219.

(28) Barckholtz, T. A.; Miller, T. A. *Int. Rev. Phys. Chem.* **1998**, *17*, 435.

(29) Kato, T.; Yoshizawa, K.; Yamabe, T. *J. Chem. Phys.* **1999**, *110*, 249.

(30) Appelgate, B. E.; Bezant, A. J.; Miller, T. A. *J. Chem. Phys.* **2001**, *114*, 4869.